Redox Biology 56 (2022) 102459

Contents lists available at ScienceDirect

Redox Biology

journal homepage: www.elsevier.com/locate/redox

# Pro-oxidative priming but maintained cardiac function in a broad spectrum of murine models of chronic kidney disease

Julia Wollenhaupt [a,1], Janina Frisch [b,1], Eva Harlacher [a], Dickson W.L. Wong [c], Han Jin [d,e], Corinna Schulte [a], Sonja Vondenhoff [a], Julia Moellmann [f], Barbara Mara Klinkhammer [c], Li Zhang [c], Adelina Baleanu-Curaj [a], Elisa A. Liehn [g,h], Thimoteus Speer [i], Andrey Kazakov [j], Christian Werner [j], Emiel P.C. van der Vorst [a,d,k,l,m], Simina-Ramona Selejan [j], Mathias Hohl [j], Michael Böhm [j], Rafael Kramann [n,o,p], Erik A.L. Biessen [d], Michael Lehrke [f], Nikolaus Marx [f], Joachim Jankowski [a,d], Christoph Maack [q], Peter Boor [c,o], Leticia Prates Roma [b,2,**], Heidi Noels [a,r,*,2]

[a] Institute for Molecular Cardiovascular Research (IMCAR), University Hospital RWTH Aachen, Aachen, Germany
[b] Department of Biophysics, Center for Integrative Physiology and Molecular Medicine, Medical Faculty, Saarland University, Center for Human and Molecular Biology, Homburg/Saar, Germany
[c] Institute of Pathology, University Hospital RWTH Aachen, Aachen, Germany
[d] Department of Pathology, Cardiovascular Research Institute Maastricht (CARIM), Maastricht University, Maastricht, the Netherlands
[e] Science for Life Laboratory (SciLifeLab), KTH Royal Institute of Technology, Stockholm, Sweden
[f] Department of Internal Medicine I, Cardiology, University Hospital RWTH Aachen, Aachen, Germany
[g] Institute for Molecular Medicine, University of South Denmark, Odense, Denmark
[h] National Institute for Pathology "Victor Babes", Bucharest, Romania
[i] Translational Cardio-Renal Medicine, Saarland University, Homburg/Saar, Germany
[j] Department of Cardiology, Angiology and Intensive Care Medicine, Saarland University Medical Centre, Homburg/Saar, Germany
[k] Interdisciplinary Centre for Clinical Research (IZKF), RWTH Aachen University, Aachen, Germany
[l] Institute for Cardiovascular Prevention (IPEK), Ludwig-Maximilians-University Munich, Munich, Germany
[m] German Centre for Cardiovascular Research (DZHK), Partner Site Munich Heart Alliance, Munich, Germany
[n] Institute of Experimental Medicine and Systems Biology, University Hospital RWTH Aachen, Aachen, Germany
[o] Department of Nephrology and Clinical Immunology, University Hospital RWTH Aachen, Aachen, Germany
[p] Department of Internal Medicine, Nephrology and Transplantation, Erasmus Medical Center, Rotterdam, the Netherlands
[q] Department of Translational Research, Comprehensive Heart Failure Center (CHFC), University Hospital Würzburg, Germany
[r] Department of Biochemistry, Cardiovascular Research Institute Maastricht (CARIM), Maastricht University, Maastricht, the Netherlands

ARTICLE INFO

*Keywords:*
Cardiomyopathy
Chronic kidney disease
Animal model
Oxidative stress
Cardiac remodeling

ABSTRACT

*Aims:* Patients with chronic kidney disease (CKD) have an increased risk of cardiovascular events and exhibit myocardial changes including left ventricular (LV) hypertrophy and fibrosis, overall referred to as 'uremic cardiomyopathy'. Although different CKD animal models have been studied for cardiac effects, lack of consistent reporting on cardiac function and pathology complicates clear comparison of these models. Therefore, this study aimed at a systematic and comprehensive comparison of cardiac function and cardiac pathophysiological characteristics in eight different CKD models and mouse strains, with a main focus on adenine-induced CKD.
*Methods and results:* CKD of different severity and duration was induced by subtotal nephrectomy or adenine-rich diet in various strains (C57BL/6J, C57BL/6 N, hyperlipidemic C57BL/6J *ApoE*$^{-/-}$, 129/Sv), followed by the analysis of kidney function and morphology, blood pressure, cardiac function, cardiac hypertrophy, fibrosis,

* Corresponding author. Institute for Molecular Cardiovascular Research (IMCAR), University Hospital RWTH Aachen, Aachen, Pauwelsstraße 30, 52074, Germany.
** Corresponding author. Department of Biophysics, Center for Integrative Physiology and Molecular Medicine, Medical Faculty, Saarland University, Center for Human and Molecular Biology, Homburg/Saar, Germany.
*E-mail addresses:* leticia.prates-roma@uks.eu (L. Prates Roma), hnoels@ukaachen.de (H. Noels).
[1] Shared first authorship.
[2] *Shared last authorship.*

https://doi.org/10.1016/j.redox.2022.102459
Received 18 July 2022; Received in revised form 24 August 2022; Accepted 24 August 2022
Available online 30 August 2022

myocardial calcification and inflammation using functional, histological and molecular techniques, including cardiac gene expression profiling supplemented by oxidative stress analysis. Intriguingly, despite uremia of variable degree, neither cardiac dysfunction, hypertrophy nor interstitial fibrosis were observed. However, already moderate CKD altered cardiac oxidative stress responses and enhanced oxidative stress markers in each mouse strain, with cardiac RNA sequencing revealing activation of oxidative stress signaling as well as anti-inflammatory feedback responses.

*Conclusion:* This study considerably expands the knowledge on strain- and protocol-specific differences in the field of cardiorenal research and reveals that several weeks of at least moderate experimental CKD increase oxidative stress responses in the heart in a broad spectrum of mouse models. However, this was insufficient to induce relevant systolic or diastolic dysfunction, suggesting that additional "hits" are required to induce uremic cardiomyopathy.

*Translational perspective:* Patients with chronic kidney disease (CKD) have an increased risk of cardiovascular adverse events and exhibit myocardial changes, overall referred to as 'uremic cardiomyopathy'. We revealed that CKD increases cardiac oxidative stress responses in the heart. Nonetheless, several weeks of at least moderate experimental CKD do not necessarily trigger cardiac dysfunction and remodeling, suggesting that additional "hits" are required to induce uremic cardiomyopathy in the clinical setting. Whether the altered cardiac oxidative stress balance in CKD may increase the risk and extent of cardiovascular damage upon additional cardiovascular risk factors and/or events will be addressed in future studies.

**Abbreviations**

| *Abbreviation* | *Meaning* |
|---|---|
| 5/6 Nx | 5/6 nephrectomy |
| 8-OHdG | 8-hydroxy-2′-deoxyguanosine |
| *Acp5* | Acid phosphatase 5 |
| AFOG | Acid Fuchsin Orange G |
| *Ager* | Advanced glycosylation end product-specific receptor |
| ALAS2 | Aminolevulinic acid synthase 2 |
| *AngII* | Angiotensin II |
| *Anp* | atrial natriuretic peptide |
| *Apln* | Apelin |
| *ApoE* | Apolipoprotein E |
| *Bnp* | Brain natriuretic peptide |
| CAT | Catalase |
| *Ccl* | CC-chemokine ligand |
| cDNA | Complementary deoxyribonucleic acid |
| *Cebpb* | CCAAT/enhancer binding protein (C/EBP), beta |
| CKD | Chronic kidney disease |
| COL | Collagen |
| CVD | Cardiovascular disease |
| *Ddit4* | DNA-damage-inducible transcript 4 |
| DEG | Differentially expressed genes |
| *Depp1* | DEPP1 autophagy regulator |
| GAPDH | Glyceraldehyde-3-phosphate dehydrogenase |
| *Gpnmb* | Glycoprotein (transmembrane) nmb |
| *GusB* | Glucuronidase beta |
| *Hba-a* | Hemoglobin alpha, adult chain |
| HE | Hematoxylin-Eosin |
| HFD | Western-type high-fat diet |
| HO-1 | Heme oxygenase 1 |
| *Hprt1* | Hypoxanthine phosphoribosyltransferase 1 |
| *Icam1* | Intercellular adhesion molecule 1 |
| *Kcne1* | Potassium voltage-gated channel, Isk-related subfamily, member 1 |
| LV | Left ventricular |
| *Mmp* | Matrix metallopeptidase |
| *Myoc* | Myocilin |
| NNT | Nicotinamide nucleotide transhydrogenase |
| NOX | NADP oxidase |
| PAS | Periodic acid-Schiff |
| PCR | Polymerase chain reaction |
| PRX | Peroxiredoxin |
| *Rgcc* | Regulator of cell cycle |
| RNA | Ribonucleic acid |
| ROS | Reactive oxygen species |
| SMA | Smooth muscle actin |
| *Smoc2* | SPARC related modular calcium binding 2 |
| *Snca* | Synuclein, alpha |
| SOD | Superoxide dismutase |
| *Sphk1* | Sphingosine kinase 1 |
| *Spon2* | Spondin 2 |
| TAC | Transversal aortic constriction |
| *Tgfb1* | Transforming growth factor beta |
| *Tnf* | Tumor necrosis factor alpha |
| TUB | Tubulin |
| WGA | Wheat germ agglutinin |

## 1. Introduction

Chronic kidney disease (CKD) is a worldwide health problem with an estimated prevalence of ~13% globally [1]. Even in early CKD stages, the risk of cardiovascular disease (CVD) is significantly enhanced [2], and this further increases in advanced stages (stage 4–5) with ~40–50% of CKD patients dying from cardiovascular complications [3]. In recent years, CKD has been identified as an independent risk factor for CVD, beyond classical cardiovascular risk factors such as age, smoking, diabetes or hypertension [4–7]. Myocardial changes in response to CKD have been summarized as 'uremic cardiomyopathy' and include inflammatory and oxidative stress responses, cardiac fibrosis and left ventricular (LV) hypertrophy [3,8].

Mouse models offer the advantage to study potential disease regulators by using genetically modified strains. Thus, a detailed characterization of available mouse models to examine CKD-associated CVD is essential for future studies aiming to unravel the molecular mechanisms underlying pathophysiological kidney-heart crosstalk. A frequently used model to induce CKD in animals is sub-total nephrectomy (5/6 Nx), which combines unilateral nephrectomy with pole resection of the other kidney and thus removes over 80% of the total kidney tissue with subsequent development of CKD. Alternatively, an adenine-supplemented diet triggers CKD through inducing tubulointerstitial nephropathy [9,10]. Both models have been employed in mice to induce CKD and to study CKD-associated CVD, however, revealed quite variable effects on

the heart [11]. This may result from differences in experimental conditions, mouse strains as well as reported parameters of cardiac function and/or remodeling. 129/Sv mice are often used to study CKD, while the C57BL/6 strain is commonly used in genetically modified models. Of note, C57BL/6J mice carry a loss-of-function mutation in the gene encoding the mitochondrial transhydrogenase (*Nnt*), a key regulator of oxidative stress through connecting the NADH with the NADPH pool in mitochondria, and might therefore display differential outcomes in terms of organ pathophysiology compared to C57BL/6 N mice [12]. Furthermore, apolipoprotein E-deficient ($ApoE^{-/-}$) mice on a high-fat diet are frequently studied to mirror the human situation with a high prevalence of hyperlipidemia as risk factor for both CKD [6] and CVD [13].

In addition to the potential impact of the mouse strain and experimental conditions on cardiac effects in CKD, the lack of consistent reporting of parameters of cardiac function and remodeling complicates a clear comparison of different studies and CKD models. CKD may affect heart function and may trigger pathophysiological responses including cardiac hypertrophy, fibrosis, calcification and inflammation. However, former studies mostly did not report on all of these parameters and often focused on selected pathophysiological processes in the heart. Furthermore, even within one study, different readouts of a pathophysiological process or cardiac function may be differentially affected, as revealed in our recent systematic review and meta-analysis [11].

Overall, studies comparing differential CKD-inducing procedures and mouse strains with a detailed systematic comparison of kidney as well as cardiac function and morphological parameters are lacking, yet are important to identify potential common pathophysiological mechanisms of CKD-associated CVD. Therefore, we aimed to perform a comparative study directly facing eight different experimental models and protocols to induce CKD in C57BL/6 (N and J), 129/Sv and hyperlipidemic $ApoE^{-/-}$ mice (Fig. 1) to expand the knowledge on strain- and protocol-specific differences in the field of cardiorenal research and to identify potential common pathways in the development of uremic cardiomyopathy.

Surprisingly, and in contrast to several previous studies, we found that despite the induction of relevant uremia in several of the employed models, neither systolic nor diastolic dysfunction or substantial structural remodeling occurred, casting doubts upon a simple mono-causal concept of uremic cardiomyopathy. However, CKD induced a pro-oxidative shift that may prime the hearts towards second hits. Whether this priming is protective or increases the susceptibility towards additional stressors needs to be clarified by future studies.

## 2. Materials and methods

Detailed description in Supplemental Methods

### 2.1. Animal experiments and organ isolation

The studies were performed with male mice, approved by local regulatory authorities (81–02.04.2017.A504; 29/2018) and performed according to local, national and European Union ethical guidelines. CKD was induced in C57BL/6J, hyperlipidemic C57BL/6J $ApoE^{-/-}$, C57BL/6 N or 129/Sv, by one-step or two-step 5/6 nephrectomy, or by feeding an adenine-supplemented diet (experimental details in Fig. 1 and Suppl. Table 1). Kidney function was assessed by measuring creatinine and urea in serum or plasma. Blood pressure measurements were performed via a

**A. CKD MODELS**

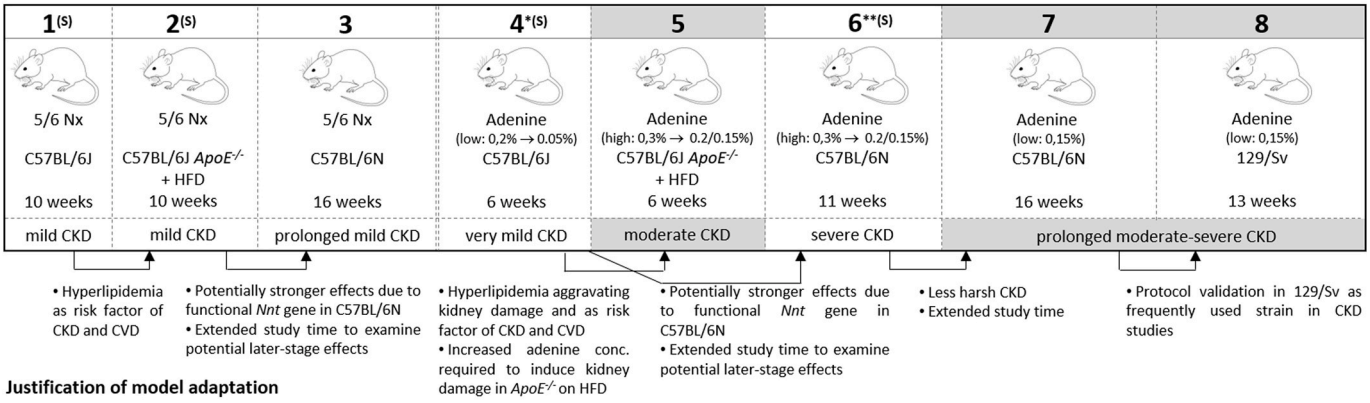


**Justification of model adaptation**

- 1(S): • Hyperlipidemia as risk factor of CKD and CVD
- 2(S): • Potentially stronger effects due to functional *Nnt* gene in C57BL/6N • Extended study time to examine potential later-stage effects
- 3: • Less harsh CKD • Extended study time
- 4*(S): • Hyperlipidemia aggravating kidney damage and as risk factor of CKD and CVD • Increased adenine conc. required to induce kidney damage in $ApoE^{-/-}$ on HFD
- 5: • Potentially stronger effects due to functional *Nnt* gene in C57BL/6N • Extended study time to examine potential later-stage effects
- 6**(S): • Less harsh CKD • Extended study time
- 7: • Less harsh CKD • Extended study time
- 8: • Protocol validation in 129/Sv as frequently used strain in CKD studies

**B. RESULTS SUMMARY**

| Model | | Kidney parameters | | | Blood pressure | | Heart parameters (hypertrophy, fibrosis, function) | Oxidative stress markers | Anti-oxidative response | Other | Figure |
|---|---|---|---|---|---|---|---|---|---|---|---|
| | | Creatinine | Urea | Fibrosis markers COL1/SMA | Systolic | Diastolic | | | | | |
| Model 1 (S) | 5/6 Nx in C57BL/6J (10 weeks) | ↗= | ↗ 1.7-fold | ↔ | ↔ | ↔ | very mild ↘ in (dP/dt)max (by 14%) under stress | | | | S1 |
| Model 2 (S) | 5/6 Nx in C57BL/6J *ApoE*$^{-/-}$ on HFD (10 weeks) | ↗= | ↗ 1.4-fold | ↔ | ↔ | ↔ | ↔ | | | | S2 |
| Model 3 | 5/6 Nx in C57BL/6N (16 weeks) | ↔ | ↗ 1.9-fold | ↔ | ↗ (by 13%) | ↗ (by 23%) | ↘ in CO (by 35%), but = EF | | | | 2, S3 |
| Model 4*(S) | Adenine (low) in C57BL/6J (6 weeks) | ↘= | ↘= | COL1 ↗ 2-fold; SMA ↔ | ↔ | ↔ | very mild ↘ in EF (by 11%) | | | | S4 |
| Model 5 | Adenine (high) in C57BL/6J *ApoE*$^{-/-}$ on HFD (6 weeks) | ↗ 1.8-fold | ↗ 2.9-fold | COL1/SMA ↗ > 5-fold | ↔ | ↔ | ↔ | ↗ 8-OHdG | | | 3, S5 |
| Model 6**(S) | Adenine (high) in C57BL/6N (11 weeks) | ↗ >14-fold | ↗ >14-fold | COL1/SMA ↗ 3- to 4-fold | ↔ | ↔ | ↔ | | | ↗ ICAM1; cardiac deposits | S6 |
| Model 7 | Adenine (low) in C57BL/6N (16 weeks) | ↗ 5.5-fold | ↗ 4.8-fold | COL1 ↗ 9-fold; SMA ↗ 3-fold | | | ↔ | ↗ HO-1; ↗ 8-OHdG (*P*=0.0729) | ↗ | ↗ ICAM1 | 4, S7 |
| Model 8 | Adenine (low) in 129/Sv (13 weeks) | ↗ 7.1-fold | ↗ 5.7-fold | COL1 ↗ 10-fold; SMA ↔ | | | ↔ (except ↗ heart rate) | ↗ HO-1 (*P*=0.057); ↗ 8-OHdG (*P*=0.0786) | ambivalent | cardiac deposits | 5, S8 |

increase
decrease
↔ unmodified

*HFD = high-fat diet*

** Model 4: Insufficient kidney damage*

***Model 6: Severe kidney damage with health impairment*

*(S) Results and figures in supplement*

**Fig. 1.** Schematic overview of studied mouse models and results summary. CKD was induced in C57BL/6J, hyperlipidemic C57BL/6J $ApoE^{-/-}$, C57BL/6 N or 129/Sv, by 5/6 nephrectomy (5/6 Nx) or by feeding an adenine-supplemented diet (diet details in Suppl. Table 1). Although overall, no cardiac dysfunction, hypertrophy or interstitial fibrosis could be observed, several weeks of at least moderate CKD did alter oxidative stress responses in the heart and enhanced cardiac oxidative stress markers in each mouse strain. 129/Sv mice with moderate to severe CKD as well as C57BL/6 N with severe CKD also developed myocardial calcified deposits surrounded by localized fibrotic tissue. *COL1 = collagen 1; CO = cardiac output; (dP/dT)max: maximum rate of left ventricular pressure rise over time (mmHg/s); EF = ejection fraction; HFD = high-fat diet; HO = heme oxygenase; ICAM = intercellular adhesion molecule; 8-OHdG = 8-hydroxy-2-deoxyguanosine; SMA = smooth muscle actin.*

non-invasive tail-cuff method. Cardiac functional measurements were performed using echocardiography and/or invasive Millar catheter analysis. At sacrifice, isolated organs were processed for histological stainings, Western blot analyses or quantitative PCR/RNA sequencing to analyze potential pathophysiological processes.

### 2.2. Western blot analyses, tissue stainings and redox analysis via roGFP2-Orp1

Tissue homogenates from explanted heart apex and kidney were analyzed by SDS-PAGE for protein expression of important regulators of oxidative stress responses (superoxide dismutase (SOD) 1, SOD2, catalase (CAT), peroxiredoxin (PRX) 2, PRX3, NADPH oxidase (NOX) 2). Also, heme oxygenase 1 (HO-1) as oxidative stress biomarker as well as collagen (COL) 1 and alpha smooth muscle actin (αSMA) as markers of organ fibrosis were quantified, using γTubulin (γTUB) or glyceraldehyde 3 phosphate dehydrogenase (GAPDH) as internal loading controls.

Cardiac transversal and kidney longitudinal tissue slices were prepared from fixed, paraffin-embedded or fresh-frozen tissue for histological and immunohistochemical analyses, including Hematoxylin-Eosin (HE), Alizarin red (cardiac calcification), Von Kossa (cardiac calcification), Picro Sirius red (cardiac fibrosis), Acid Fuchsin Orange G (AFOG, renal fibrosis), periodic acid-Schiff (PAS, renal tubular injury), 8-hydroxy-2′-deoxyguanosine (8-OHdG, cardiac DNA oxidation) and wheat germ agglutinin (WGA, cardiac membranes for hypertrophy analysis).

*In vivo* oxidative stress was mapped using a transgenic mouse model expressing the $H_2O_2$ sensor roGFP2-Orp1 (Model 7), with the mitochondrial redox state in fixed frozen cardiac tissue sections analyzed through fluorescence analysis.

### 2.3. Quantitative PCR analysis and RNA sequencing

Apical sections of the hearts were processed for RNA isolation, cDNA synthesis and quantitative real-time PCR according to standard protocols, analyzing markers for hypertrophy (atrial natriuretic peptide (*Anp*), brain natriuretic peptide (*Bnp*)), fibrosis (collagen 3a1 (*Col3a1*), collagen 1a1 (*Col1a1*), transforming growth factor beta (*Tgfb1*)) and inflammation (CC-chemokine ligand 2 (*Ccl2*), tumor necrosis factor alpha (*Tnf*), intercellular adhesion molecule 1 (*Icam1*)). Hypoxanthine phosphoribosyltransferase 1 (*Hprt1*) and glucuronidase beta (*GusB*) or glyceraldehyde 3 phosphate dehydrogenase (*Gapdh*) were used as internal controls.

Paired-end RNA sequencing was performed at Genewiz (GENEWIZ GmbH, Germany) using Illumina NovaSeq 6000 with included quality controls. Sequences were aligned to the reference mouse genome GRCm38.p6. Gene-level read counts were quantified and assembled using the R package Rsubread followed by differential expression analysis carried out using the R package DESeq2. This revealed differentially expressed genes (DEGs) between Sham and Adenine groups, with *P*-values further adjusted ($p_{adjusted}$) by the Benjamini-Hochberg procedure. Data were visualized in a volcano plot and using two independent approaches, significant DEGs ($\log_2$(fold change) $> 1$ or $< -1$, $p_{adjusted} < 0.05$) were stratified based on their involvement in enriched and pathology-relevant gene ontology terms, revealing a top 10 DEG list for up- and downregulated genes (for details see Supplemental Methods). RNAseq data in this study have been deposited into Gene Expression Omnibus (GEO) and can be accessed under the accession number GSE191122.

### 2.4. Statistics

Data are presented as means ± SD. All statistical data analyses and graph preparation were performed using GraphPad Prism (Version 9). Statistics included mixed-effects analysis with Sidak's post-test for multiple comparison of matching values; two-way ANOVA with Sidak's post-test for multiple comparison without matching values; student's t-test (unpaired, two-tailed) for two-group comparisons with normal distribution and without timing variables, with additional Welsh's correction in case of non-equal standard deviation; and Mann-Whitney test for two-group comparisons without normal distribution. Outlier exclusion was performed based on the Grubbs' test in GraphPad. *P* values are defined as follows: $^*P < 0.05$, $^{**}P < 0.01$, $^{***}P < 0.001$.

## 3. Results

### 3.1. Sub-total nephrectomy (5/6 Nx) in mouse strains C57BL/6J, C57BL/6J ApoE$^{-/-}$ and C57BL/6 N (Models 1–3)

Model 1–2: We first examined 5/6 Nx-induced kidney disease and resultant cardiac effects in wild-type C57BL/6J mice as the most commonly used C57BL/6 genetic background. Overall, 10 weeks 5/6 Nx only induced a mild CKD with a minor effect on cardiac contractility under dobutamine-stress, though without clear characteristic molecular effects in the heart (Fig. 1A: Model 1; Fig. S1). Given that hyperlipidemia is a risk factor of both CKD [6] and CVD [13], we next investigated C57BL/6J *ApoE*-deficient (*ApoE*$^{-/-}$) mice on Western-type high-fat diet (HFD) for CKD-associated CVD (Fig. 1A: Model 2; Fig. S2). Also here, 10 weeks 5/6 Nx only induced a mild kidney function impairment, though without functional or molecular cardiac alterations. Results of both models are described in detail in Suppl. Results.

Model 3: C57BL/6J mice carry a loss-of-function mutation in the *Nnt* gene, which protects from pressure overload-induced oxidative stress and maladaptive cardiac remodeling [12]. Therefore, in a third model, 5/6 Nx was investigated using C57BL/6 N mice, which express an intact *Nnt* gene [12]. CKD was extended up to 16 weeks after surgery to examine potential later-stage effects, with no mortality observed after surgery (Fig. 1A/2A: Model 3). Despite an early drop in body weight of both sham- and 5/6 Nx groups, all animals started to gain weight from post-operative day 7 on (Fig. 2B). Although plasma creatinine was not significantly different at the endpoint, 5/6 Nx significantly increased plasma urea values ~1.9-fold compared to controls (Fig. 2C). Histological analysis of remnant kidneys revealed no glomerular damage, but focal fibrosis with immune cell infiltration in all C57BL/6 N mice with CKD (AFOG and PAS staining: Fig. 2D), however, without significant effect on overall protein levels of COL1 or αSMA in the kidney (Fig. S3A). Although ejection fraction was unchanged at the endpoint, cardiac output was reduced by ~35%, accompanied by slightly decreased (though insignificant) changes in LV end-diastolic volume (Fig. 2E; Suppl. Table 2). All further cardiac functional parameters did not show significant changes (Suppl. Table 2). Despite reduced cardiac output, diastolic and systolic blood pressure were mildly increased (by 23%, respectively, 13%) in 5/6 Nx mice at the endpoint (Fig. 2F, Fig. S3B), indicating an increase in systemic vascular resistance. Analyses of cardiac hypertrophy markers revealed neither changes in *Anp* or *Bnp* mRNA expression nor in heart weight per tibia length, while cardiomyocyte diameter was even slightly reduced in CKD vs. control animals (Fig. 2G; Figs. S3C–D). Alizarin Red staining for calcification could not reveal any calcification deposits in either group (Fig. S3E). An increase in cardiac fibrosis by 5/6 Nx as detected by Sirius Red staining resulted rather from a pericardial fibrous layer instead of revealing changes in interstitial or perivascular fibrosis (Fig. 2H). In line, cardiac mRNA expression of pro-fibrotic genes (*Tgfb1*, *Col1a1* and *Col3a1*: Fig. 2I) as well as western blot analyses of fibrosis-related protein expression (COL1, αSMA: *data not shown*) did not reveal changes upon 5/6 Nx. Furthermore, no induction of cardiac inflammatory processes was detected in 5/6 Nx compared to sham-operated mice (*Tnf*, *Ccl2, Icam1:* Fig. 2I).

In summary, prolonged mild kidney damage by 5/6 Nx in C57BL/6 N mice induced a blood pressure increase accompanied by mild cardiac dysfunction, while no cardiac hypertrophy, calcification, inflammation or cardiac interstitial fibrosis were observed.

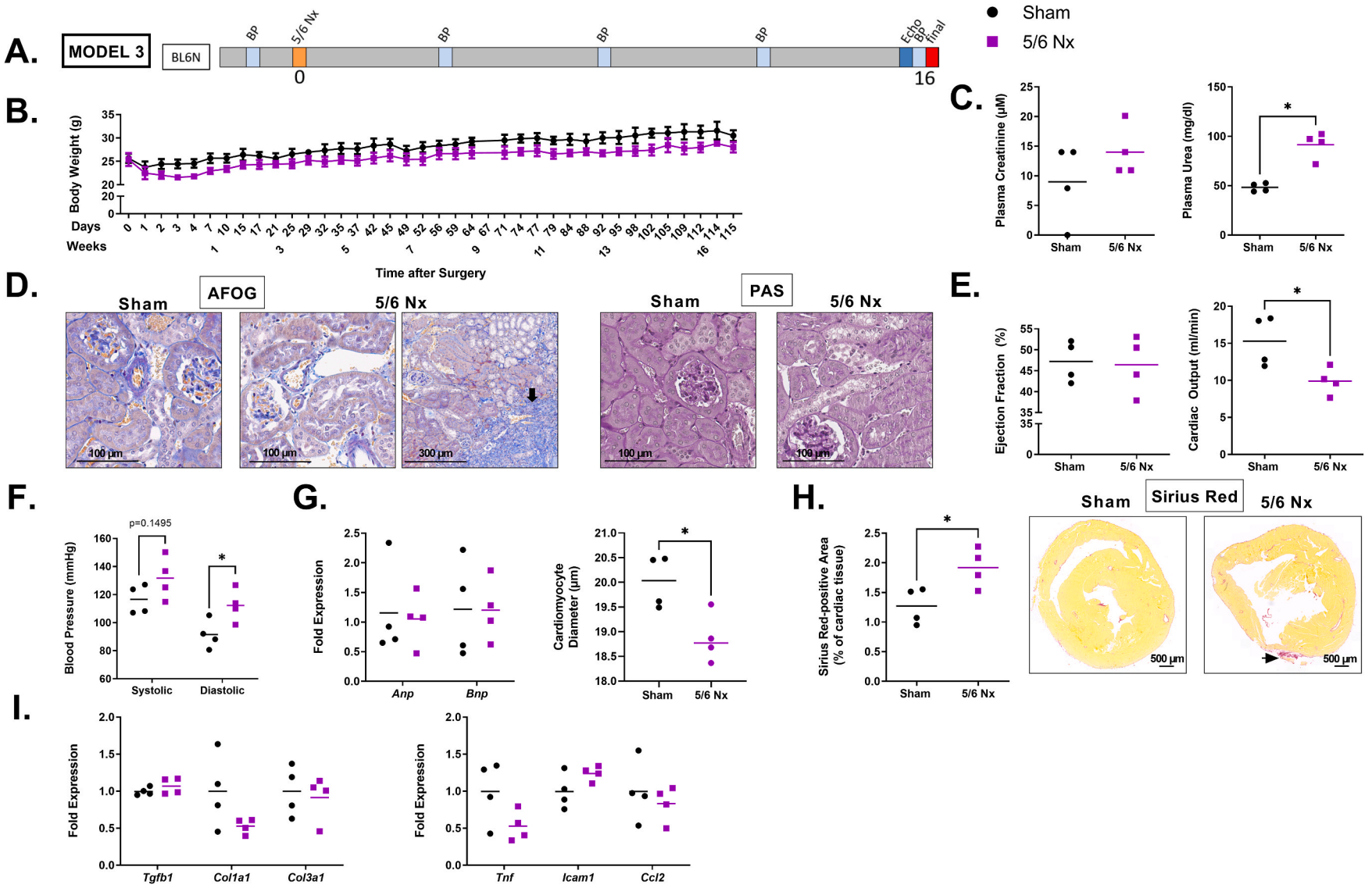


**Fig. 2.** MODEL 3–5/6 Nx in C57BL/6 N mice. A) Experimental timeline. BL = baseline. BP = blood pressure. B) Body-weight curve (Sham n = 4; 5/6 Nx n = 4). C) Plasma creatinine and urea. D) Representative images of kidney AFOG and PAS staining. E) Ejection fraction and cardiac output via echocardiography. F) Systolic and diastolic blood pressure at the endpoint. G) Analysis of *Anp/Bnp* gene expression in cardiac tissue (normalized to *Gapdh*) and cardiomyocyte diameter in WGA-stained cardiac sections. H) Quantification and representative images of histological Sirius Red staining of cardiac sections. I) Quantitative PCR on cardiac tissue for markers of fibrosis (*Tgfb1, Col1a1, Col3a1*) and inflammation (*Tnf, Icam1, Ccl2*), normalized to *Hprt1* and *GusB*. B–I) Unless otherwise indicated, endpoint analyses were performed and data are presented as means ± SD or dot plots. *p < 0.05 comparing nephrectomy to sham animals using mixed-effects analysis with matching values and Sidak's post-test (B), two-tailed *t*-test (parametric data; with Welch's correction in case of non-equal SDs) or Mann-Whitney test (non-parametric data) (C–J). (For interpretation of the references to colour in this figure legend, the reader is referred to the Web version of this article.)

### 3.2. Adenine diet using mouse strains C57BL/6J, C57BL/6J ApoE$^{-/-}$, C57BL/6 N and 129/Sv (Models 4–8)

Model 4: CKD can also be induced by adenine-feeding, triggering tubulointerstitial nephropathy [9,10], with the advantage that adapting the adenine concentration enables the induction of different degrees of CKD. Feeding C57BL/6J mice a low concentrated adenine diet for 6 weeks (2 weeks 0.2% + 4 weeks 0.05%) led only to a very mild kidney damage (Fig. 1A: Model 4; Fig. S4). Although echocardiography revealed a mild reduction in cardiac ejection fraction at the endpoint, the absence of a sufficient chronic kidney dysfunction disqualified this model for studying the kidney-heart crosstalk.

Model 5: Following the same strategy as previously for 5/6 Nx, we next examined adenine-induced CKD in C57BL/6J *ApoE*$^{-/-}$ mice fed a HFD. Surprisingly, initial experiments revealed that - in contrast to wild-type C57BL/6J on two-weeks standard diet supplemented with 0.2% adenine (Model 4) - a HFD supplemented with 0.2% adenine did not impact the kidney in *ApoE*$^{-/-}$ mice after a two-week induction phase, as revealed by a lack of creatinine or urea increase in serum as well as by a very low degree of kidney damage and inflammation in histological analyses *(data not shown)*. Thus, for Model 5, the adenine concentration was increased to 0.3% in a 10 days-induction phase and to 0.15% in the maintenance phase for 4.5 weeks (Fig. 1A/3A: Model 5; diet details in Suppl. Table 1). Although this triggered weight reduction towards the end of the induction phase, switching to 0.15% adenine stabilized weight and even allowed weight gain towards the end of the experiment, though weight remained significantly lower compared to the control group, though without mortality observed in either group (Fig. 3B). Adenine-fed *ApoE*$^{-/-}$ mice presented a 1.8-fold, respectively, 2.9-fold increase in serum creatinine and urea levels at the endpoint, a high degree of kidney fibrosis, severe tubular injury and inflammatory cell infiltration, as well as >5-fold increased protein expression of COL1 and αSMA in the kidney, confirming nephropathy (Fig. 3C–E; Fig. S5B). Nonetheless, Millar catheter analysis as well as echocardiography could not reveal effects on heart function at 6 weeks (Fig. 3F and G, Suppl. Table 2–3), nor at two or four weeks after the start of adenine feeding (by Millar catheter analysis; *data not shown*). Also, no effects were observed on end-point systolic or diastolic blood pressure (Fig. S5A). Heart weight normalized to tibia length *(data not shown)* and cardiac gene expression profiling of hypertrophy markers (*Anp*, *Bnp*) were unchanged, while cardiomyocyte diameter showed a small decrease (3.8% vs. control) (Figs. S5C–D). Sirius Red staining with quantification of interstitial fibrosis in the heart revealed no alterations in CKD, in line with an unaltered expression of genes involved in fibrosis (*Col1a1*, *Col3a1*, *Tgfb1*; Fig. S5C/E). No cardiac calcification could be detected in CKD by Alizarin Red staining (*data not shown*). Furthermore, gene expression profiling could not reveal an increased inflammatory response in the hearts of CKD mice (Fig. S5C). In our hands, this being the first CKD model that revealed a stable, >2.5-fold increase in serum urea levels, a steady increase in serum creatinine as well as moderate kidney damage, we additionally analyzed in this model oxidative stress responses in the heart. Although antioxidative enzymes and oxidative stress markers NOX2 and HO-1 were unaltered in CKD mice (Fig. 3H; Fig. S5F), staining for 8-OHdG showed significantly increased DNA oxidation as marker of oxidative stress in the adenine-fed group (Fig. 3I, Fig. S5G).

Altogether, this adenine model induced a stable moderate CKD in *ApoE*-deficient animals, and although no effects on cardiac function could be observed, increased oxidative stress was revealed in the heart.

Model 6: Next, similarly as previously for 5/6 Nx, we also examined high adenine-induced CKD in C57BL/6 N mice (Fig. 1A/S6A: Model 6; diet details in Suppl. Table 1). However, serious body-weight loss of the adenine mice immediately after starting the feeding with further progression of weight loss over time necessitated termination of the experiment after 11 weeks. Kidney and cardiac analysis revealed a strong degree of kidney dysfunction and clear macroscopic cardiac modifications visible as white myocardial deposits, yet without functional cardiac impairment, cardiac hypertrophy or interstitial fibrosis (Fig. S6). Since the extensive body and heart-weight loss were expected to impact on the results, this model was concluded as unsuitable for further investigation.

Model 7: Aiming at a less harsh but prolonged adenine-induced CKD exposure, C57BL/6N-roGFP2-Orp1 mice, which express the $H_2O_2$ sensor roGFP-Orp1, were fed with a constant low-dose adenine (0.15%) [14] (Fig. 1A/4A: Model 7; diet details in Suppl. Table 1) for 16 weeks. Adenine-fed mice revealed comparable weight gains as control mice until week 8, followed by slow but continuous weight loss, but no mortality, until 16 weeks of adenine-feeding (Fig. 4B). CKD onset and progression were confirmed by enhanced creatinine plasma values from week 9 after diet start, which further increased over time (to ~5.5-fold increase at the endpoint; Fig. 4C). Plasma urea levels were similarly increased (to ~4.8-fold increase at the endpoint; Fig. 4C). Broad kidney damage was confirmed by significantly increased renal COL1 and αSMA protein expression in adenine-fed mice, accompanied by histological detection of extensive kidney fibrosis with widespread immune cell infiltration, although with only low to moderate tubular injury (Fig. 4D; Fig. S7B). Echocardiography did not reveal impaired cardiac function after 16 weeks of adenine-feeding (Fig. 4E, Suppl. Table 2) and BNP plasma concentration was not altered (Fig. S7A). *Anp* or *Bnp* cardiac mRNA expression, cardiomyocyte diameter and heart weight remained unchanged, suggesting no hypertrophic response in this model (Fig. 4F; Figs. S7C–D). Furthermore, CKD did not induce cardiac fibrosis (*Tgfb1, Col1a1*, *Col3a1;* Sirius Red staining) nor calcification (Alizarin Red staining) (Fig. 4G; Figs. S7E–F).

However, analysis of pro-inflammatory cardiac gene expression revealed significantly increased *Icam1* in CKD animals vs. controls, though without effects on *Tnf* or *Ccl2* (Fig. 4G). Although quantification of mitochondrial roGFP2-Orp1 signal could not detect a clear increase in free $H_2O_2$ sensed by the reporter (Fig. 4H and I), adenine-induced CKD did alter oxidative stress responses in the heart, with a significant increase in cytosolic SOD1 and mitochondrial SOD2 expression as well as increased levels of HO-1 protein and DNA oxidation as oxidative stress markers (Fig. 4J and K; Figs. S7G–H).

In summary, prolonged moderate to severe kidney impairment in this model did not impact directly on cardiac function or morphology, but increased oxidative stress in the heart

Model 8: In order to exclude mouse strain-specific effects, the last adenine protocol from Model 7 was also applied to 129/Sv mice, a mouse strain frequently used in CKD research (Fig. 1A/5A: Model 8; diet details in Suppl. Table 1). The body-weight of the adenine group was stable until week 6, but the experiment was terminated at 13 weeks due to health condition and threshold-crossing body-weight loss (Fig. 5B). CKD onset and progression upon adenine diet were confirmed by increasing plasma creatinine and urea levels over time (Fig. 5C; to ~6-7-fold increase at endpoint) as well as strong kidney fibrosis as detected by increased COL1 protein expression (Fig. S8A), renal Sirius Red staining *(data not shown)* and AFOG staining (Fig. 5D). Furthermore, tubular injury was detected in all adenine-fed mice in PAS-stained histological slides (Fig. 5D). Cardiac functional analyses via echocardiography did not show significant changes for any evaluated parameter except for increased heart rate (Fig. 5E, Suppl. Table 2). BNP plasma levels tended to increase at the endpoint (Fig. S8B), but no statistically significant differences could be detected for cardiac hypertrophy-related readouts, as *Bnp/Anp* cardiac mRNA, cardiomyocyte diameter nor heart weight (Fig. 5F; Figs. S8C–D). Of note, similar to model 6 of severe CKD in C57BL/6 N, mainly apical myocardial deposits were visible in all adenine-fed but not in control mice (Fig. 5G). These deposits were present as localized spots of strong calcification and fibrosis, with variable size among CKD animals (representative histological images, Fig. 5G (large deposits), Fig. S8E (small deposits)). Furthermore, interstitial cardiac fibrosis was detected in both control and adenine-fed mice, though without significant differences detected by Sirius Red

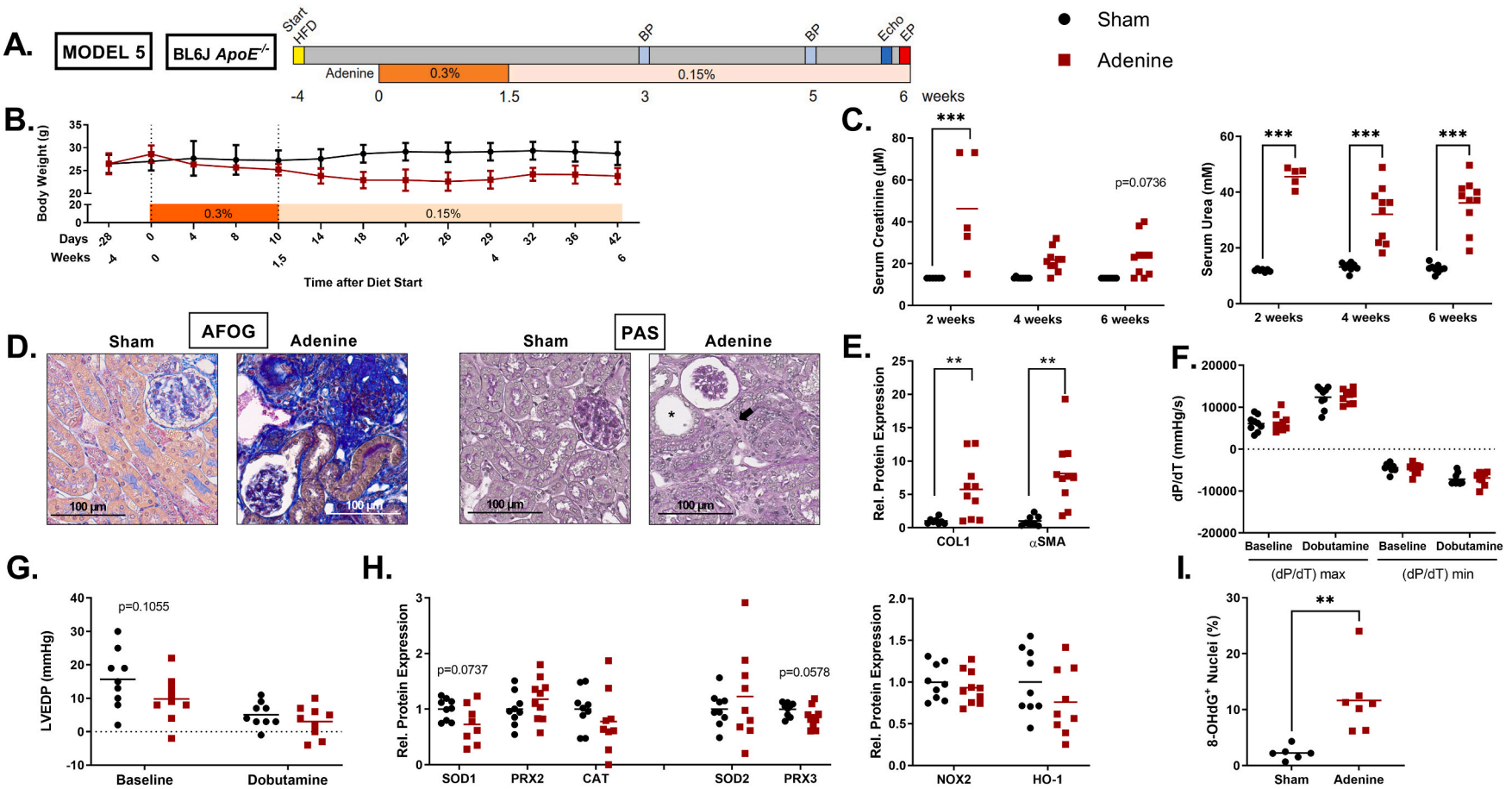


**Fig. 3.** MODEL 5 - High-dose Adenine diet in C57BL/6J *ApoE* $^{-/-}$ mice. A) Experimental timeline. HFD = high fat diet, BP = blood pressure, EP = endpoint. B) Body-weight curve (Sham n = 9; Adenine n = 10). C) Serum creatinine and urea, measured at 2, 4 and 6 weeks. D) Representative images of kidney AFOG and PAS staining (PAS: asterisk indicates tubular injury; arrow indicates infiltrating cells). E) Quantitative analysis of COL1 and αSMA as fibrosis markers in kidney tissue via western blot, normalized to loading control GAPDH. F) Invasive heart function analysis at endpoint by Millar catheter: (dP/dT) max and min. G) Left ventricular end diastolic pressure (LVEDP). H) Quantitative analysis of cytosolic (SOD1, PRX2, CAT) and mitochondrial (SOD2, PRX3) antioxidative enzyme expression as well as oxidative stress markers (NOX2, HO-1) in heart tissue lysates via western blot, normalized to loading control (GAPDH or γTUB). I) 8-OHdG immunostaining in heart sections. B-I) Shown are means ± SD or dot plots. *p < 0.05, **p < 0.01, p***<0.001 comparing adenine to sham animals using two-way ANOVA and Sidak's post-test (B–C, F-G), two-tailed *t*-test (parametric data; with Welch's correction in case of non-equal SDs) or Mann-Whitney test (non-parametric data) (E, H–I).

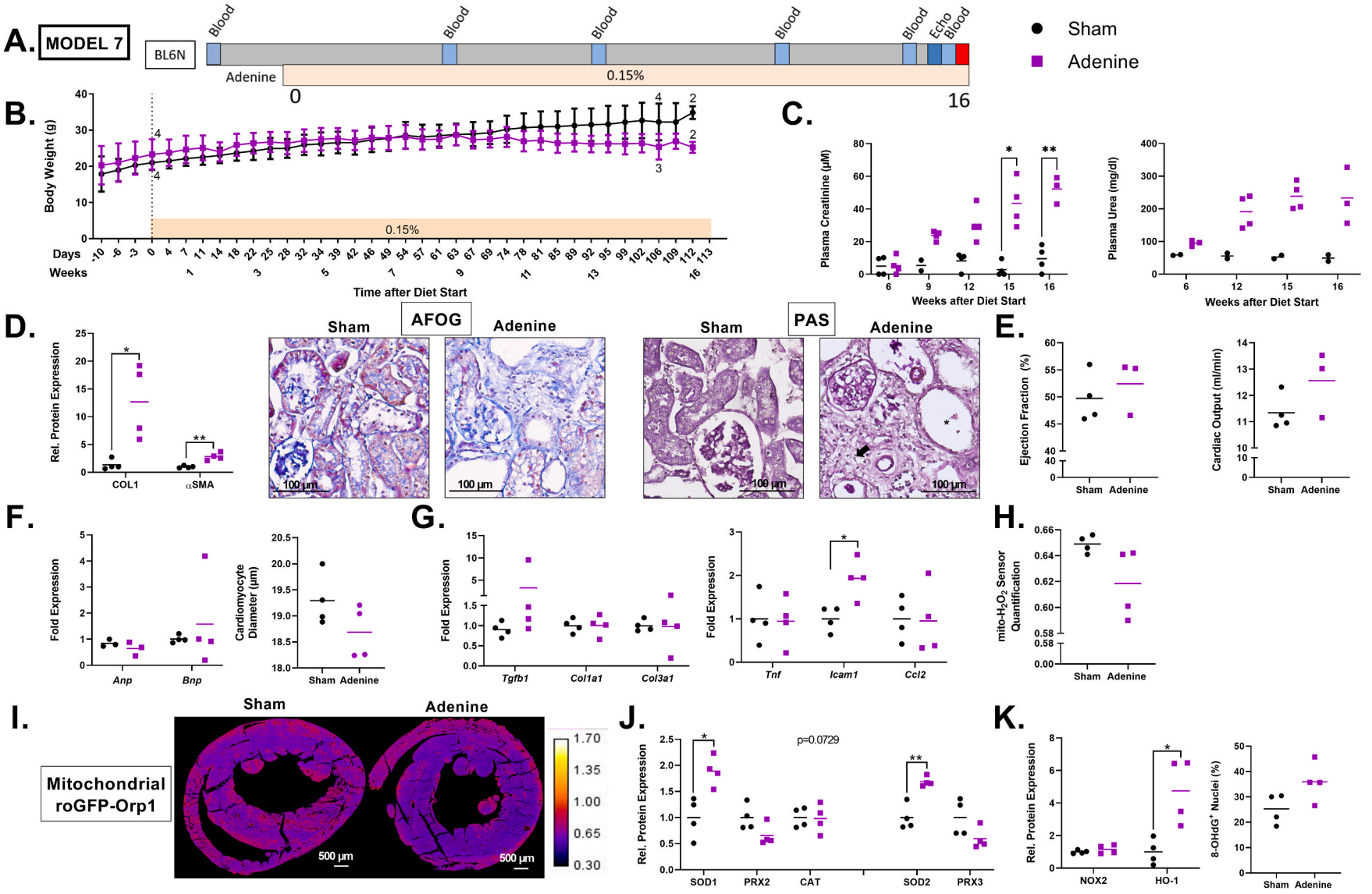


**Fig. 4.** MODEL 7 - Low-dose Adenine diet in C57BL/6 N mice. A) Experimental timeline. BL = baseline. B) Body-weight curve (Sham n = 4; Adenine n = 4). C) Plasma creatinine and urea measured at 6, 9, 12, 15 and 16 weeks (missing values due to insufficient blood collection and no 9 weeks data for urea due to limited blood availability). D) Quantitative analysis of COL1 and αSMA as fibrosis markers in kidney tissue via western blot, normalized to loading control GAPDH, and representative images of kidney AFOG and PAS staining (PAS: asterisk indicates tubular injury; arrow indicates infiltrating cells). E) Ejection fraction and cardiac output via echocardiography. F) Cardiac analysis of *Anp/Bnp* expression (normalized to *Gapdh*) and cardiomyocyte diameter in WGA-stained cardiac sections. One *Anp* outlier excluded in Adenine group based on the Grubb's test. G) Quantitative PCR on cardiac tissue for markers of fibrosis (*Tgfb1, Col1a1, Col3a1*) and inflammation (*Tnf, Icam1, Ccl2*), normalized to *Hprt1* and *GusB*. H) Ratiometric (405 nm/488 nm) mitochondrial redox analysis in the heart (roGFP2-Orp1) at 16 weeks. I) Representative images of ratiometric (405 nm/488 nm) mitochondrial redox analysis in heart sections. J) Quantitative analysis of cytosolic (SOD1, PRX2, CAT) and mitochondrial (SOD2, PRX3) antioxidative enzyme expression in heart tissue lysates via western blot, normalized to loading control (GAPDH or γTUB). K) Quantification of oxidative stress markers via western blot (NOX2, HO-1), normalized to loading control (GAPDH or γTUB) and cardiac 8-OHdG immunostaining. B–K) Unless otherwise indicated, endpoint analyses were performed and data are presented as means ± SD or dot plots. For mice sacrificed prematurely at day 109 or day 112, kidney and heart were still collected for organ analysis of the endpoint (day 113). *p < 0.05, **p < 0.01 comparing adenine to sham animals using mixed-effects analysis with matching values and Sidak's post-test (B–C; no statistical evaluation for groups with n = 2 only), two-tailed *t*-test (parametric data; with Welch's correction in case of non-equal SDs) or Mann-Whitney test (non-parametric data) (D–K).

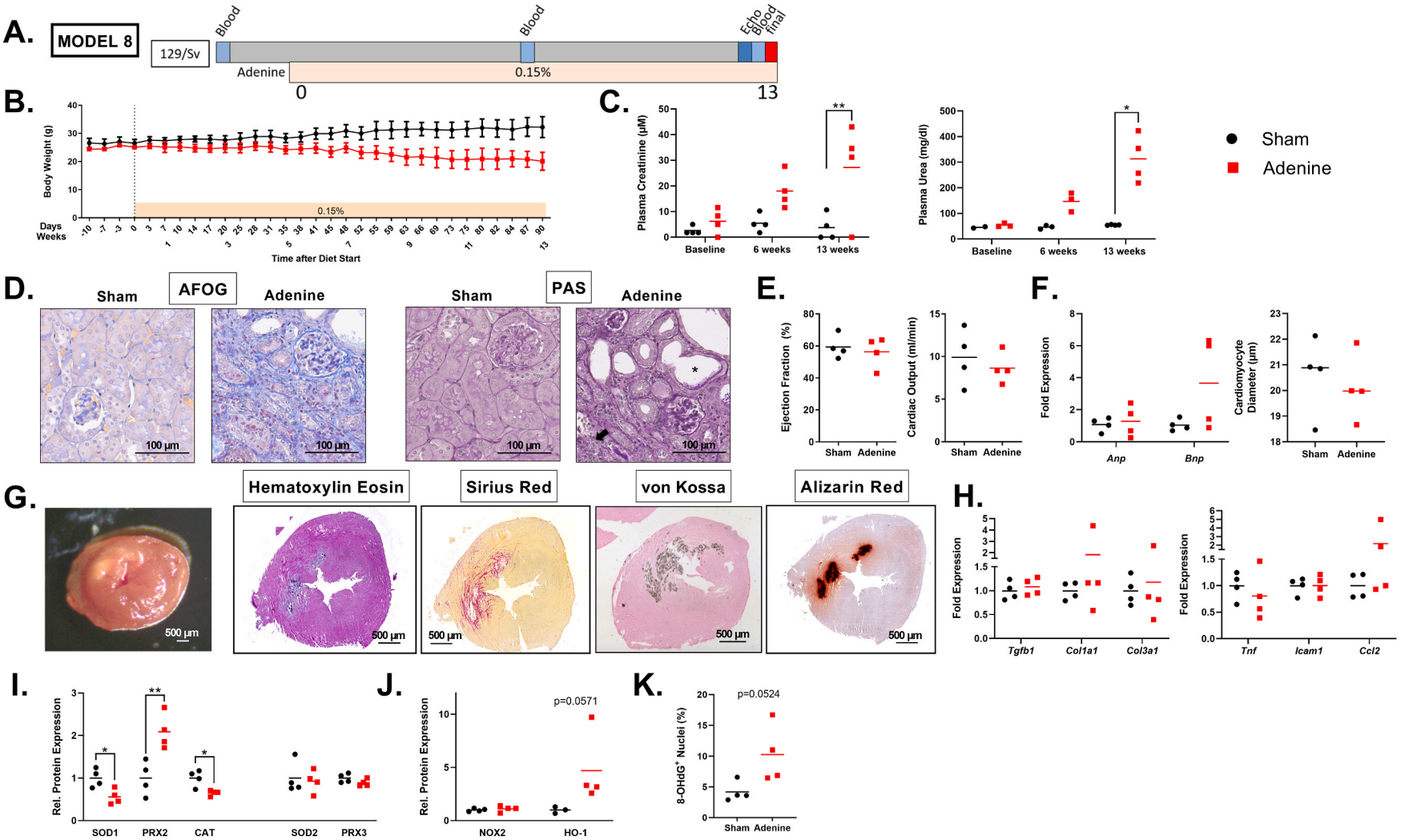


**Fig. 5.** MODEL 8 - Low-dose Adenine diet in 129/Sv mice. A) Experimental timeline. BL = baseline. B) Body-weight curve (Sham n = 4; Adenine n = 4). C) Plasma creatinine and urea. D) Representative images of kidney AFOG and PAS staining (PAS: asterisk indicates tubular injury; arrow indicates infiltrating cells). E) Ejection fraction and cardiac output via echocardiography. F) Cardiac analysis of *Anp/Bnp* expression (normalized to *Gapdh*) and cardiomyocyte diameter in WGA-stained cardiac sections. G) Representative images of adenine-induced myocardial deposits: macroscopic view, hematoxylin-eosin, Sirius Red, von Kossa and Alizarin Red stainings. H) Quantitative PCR on cardiac tissue of markers for fibrosis (*Tgfb1, Col1a1, Col3a1*) and inflammation (*Tnf, Icam1, Ccl2*), normalized to *Hprt1* and *GusB*. I) Quantitative analysis of cytosolic (SOD1, PRX2, CAT) and mitochondrial (SOD2, PRX3) antioxidative enzyme expression in heart tissue lysates via western blot, normalized to loading control (GAPDH or γTUB). J) Quantitative analysis of oxidative stress markers (NOX2, HO-1) in heart tissue lysates via western blot, normalized to corresponding loading controls (GAPDH or γTUB). K) Quantification of 8-OHdG immunostaining in heart sections. B-K) Unless otherwise indicated, endpoint analyses were performed and data are presented as means ± SD or dot plots. *p < 0.05, **p < 0.01 comparing adenine to sham animals using mixed-effects analysis with matching values and Sidak's post-test (B–C), two-tailed *t*-test (parametric data; with Welch's correction in case of non-equal SDs) or Mann-Whitney test (non-parametric data) (E–K). (For interpretation of the references to colour in this figure legend, the reader is referred to the Web version of this article.)

quantification (Fig. S8F). In contrast to these local deposits, overall COL1 or αSMA protein expression were not changed when analyzing cardiac tissue globally *(data not shown)*, and neither were cardiac expression profiles of inflammatory and pro-fibrotic genes (Fig. 5H). Cardiac expression of antioxidant enzymes was ambivalent, showing cytosolic SOD1 and CAT to be significantly decreased, while PRX2 was increased (Fig. 5I, Fig. S8G). Mitochondrial antioxidant enzyme expression profiles (SOD2, PRX3) were unmodified (Fig. 5I, Fig. S8G).

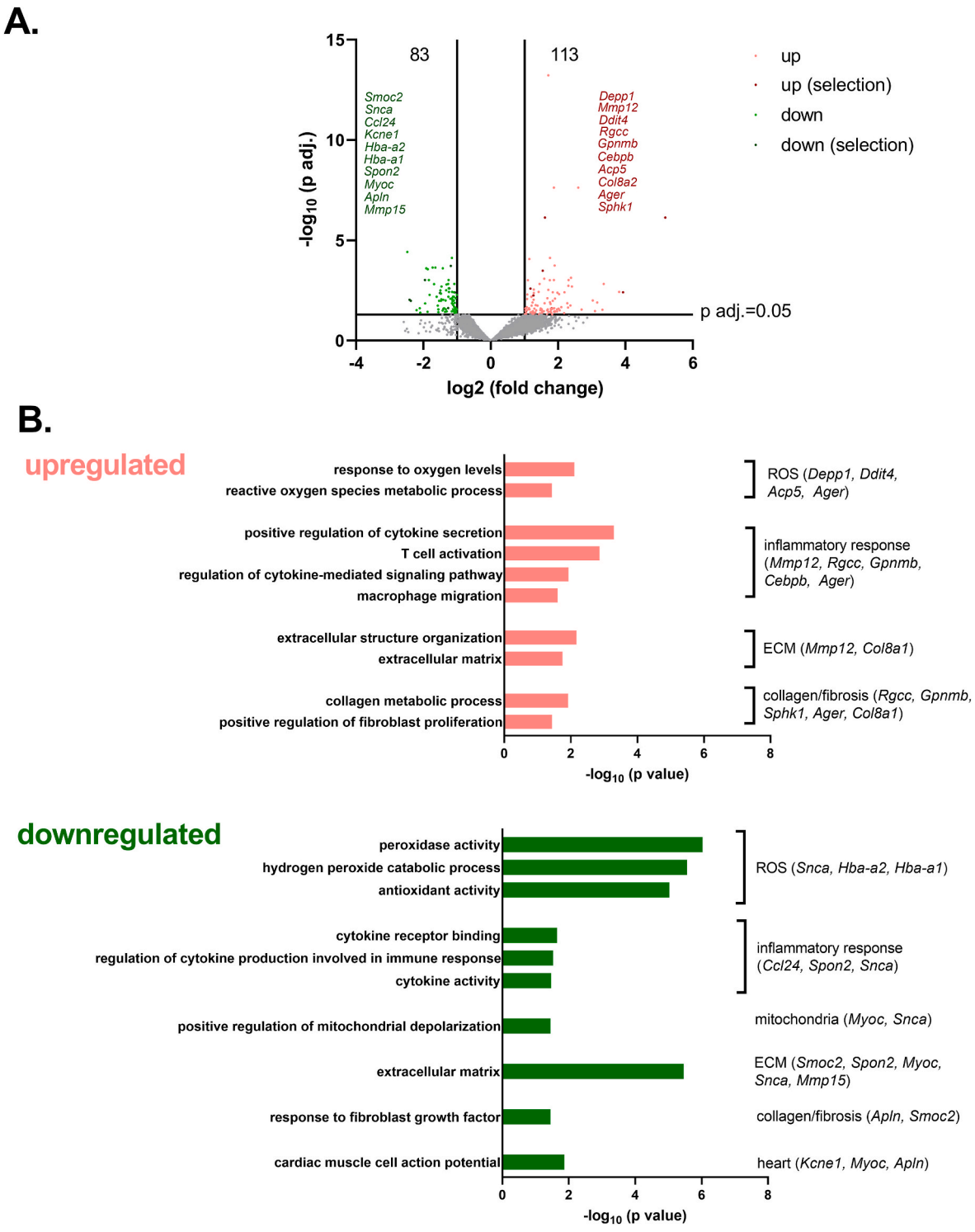


**Fig. 6.** RNA-sequencing reveals pathology-relevant molecular changes in the heart in 129/Sv mice with CKD. RNA-sequencing was performed on cardiac tissue of 129/Sv mice in CKD versus control conditions (Model 8). A) Volcano plot depicting $\log_2$(fold change) and $-\log_{10}(p_{adjusted})$ of genes, comparing the adenine-treated group to controls. Differentially expressed genes (DEGs) with $p_{adjusted} < 0.05$ and $\log_2$(fold change) $> 1$ or $< -1$ were considered as significant for further analysis, and are marked in green (downregulated) or red (upregulated); ten significantly up- and downregulated genes of interest were highlighted (green: downregulated genes; red: upregulated genes). B) Representation of enriched and pathology-relevant gene ontology (GO) terms based on the significant DEGs. Green bars indicate downregulated and red bars upregulated pathways. Selected significant DEGs associated with these GO terms are indicated. *ECM = extracellular matrix; ROS = reactive oxygen species. (For interpretation of the references to colour in this figure legend, the reader is referred to the Web version of this article.)*

Nonetheless, hearts of 129/Sv mice with adenine-induced CKD showed a trend towards increased levels of HO-1 protein and DNA oxidation by 8-OHdG staining as markers of enhanced oxidative stress (Fig. 5J–K, Figs. S8G–H).

All combined, this CKD model in 129/Sv mice induced a chronic, moderate to severe kidney dysfunction, accompanied by myocardial deposits that are associated with very local calcification and fibrosis, though without an overall increase in interstitial cardiac fibrosis. Furthermore, although cardiac function was not impaired, CKD mice displayed increased levels of oxidative stress readouts in the heart, resembling previous observations in adenine-fed C57BL/6J *ApoE*$^{-/-}$ (Model 5) and C57BL/6 N mice (Model 7).

To provide further insights into CKD-induced cardiac changes on a molecular level, RNA-sequencing was performed on cardiac tissue of adenine-fed 129/Sv mice compared to controls (Model 8). This revealed 113 significantly up-regulated and 83 down-regulated genes ($\log_2$(fold change) $> 1$ or $< -1$; adjusted p-value ($p_{adjusted}$) $< 0.05$; Fig. 6A). From each group, differentially expressed genes (DEGs) with $P_{adjusted} < 0.05$ were stratified based on their involvement in enriched and pathology-relevant gene ontology (GO) terms (see detailed description in Suppl. Methods), revealing the top 10 DEG hits annotated in Fig. 6A. Upregulated DEGs were associated with GO terms related to ROS (*Depp1, Ddit4, Ager, Acp5*), inflammatory response (*Ager, Rgcc, Mmp12, Gpnmb, Cebpb*), extracellular matrix (*Mmp12, Col8a1*) and collagen/fibrosis (*Rgcc, Gpnmb, Sphk1, Ager, Col8a1*) (Fig. 6B, upregulated). Similarly, downregulated DEGs were associated with GO terms as ROS (*Snca, Hba-a1, Hba-a2*), inflammatory response (*Ccl24, Spon2, Snca*), mitochondria (*Myoc, Snca*), extracellular matrix (*Smoc2, Spon2, Myoc, Snca, Mmp15*), collagen/fibrosis (*Apln, Smoc2*) and heart (*Kcne1, Myoc, Apln*) (Fig. 6B, downregulated).

Based on the identified functions of the dysregulated genes, the CKD hearts displayed an increased cardiac oxidative stress response characterized by an increase in ROS-inducing mediators (e.g. increased *Depp1* [15], *Ddit4* [16], *Ager* [17,18], *Sphk1* [19]). Although also protective anti-inflammatory feedback responses were detected (e.g. increased *Acp5* [20], *Mmp12* [21]), increased cardiac levels of the oxidative stress markers HO-1 and 8-OHdG pointed to an overall shift towards a pro-oxidative milieu in the heart (Fig. 7). Furthermore, an increase in pro-fibrotic mediators (*Rgcc* [22], *Ager* [23], *Col8a2* [24], *Mmp12* [25]) as well as a decrease in such mediators (*Smoc2* [26,27]) was identified by RNA-sequencing, though with the overall imbalance being insufficient to induce global cardiac interstitial fibrosis in the CKD hearts of these mice.

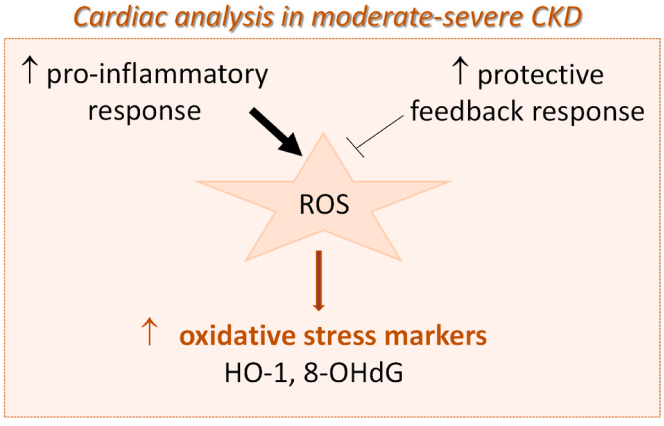


**Fig. 7.** Molecular adaptation of the heart in CKD. 129/Sv mice on adenine-induced CKD revealed an increased cardiac oxidative stress response characterized by an increase in ROS-inducing mediators and a decrease in cardioprotective mediators, as identified by RNA-sequencing. On the other hand, also protective anti-inflammatory feedback responses were detected. Overall, cardiac levels of the oxidative stress markers HO-1 and 8-OHdG were increased. Since oxidative stress signaling can both offer protective as well as detrimental effects, future studies should address whether this oxidative signature provides a certain degree of cardioprotection or in fact increases the risk of enhanced cardiovascular damage upon additional cardiovascular risk factors and/or events.

## 4. Discussion

Given the high clinical relevance of CVD in CKD [3], this study systematically and comprehensively studied cardiac function and pathophysiological characteristics of uremic cardiomyopathy in different mouse models of CKD. Intriguingly, despite the development of mild to moderate-severe CKD, neither cardiac dysfunction, hypertrophy nor interstitial fibrosis were observed. However, already moderate CKD induced a pro-oxidative shift in the heart, together with alterations in expression of various regulators of ROS formation, elimination and signal transduction. Future studies should address whether this in fact increases the risk of enhanced cardiovascular damage upon additional cardiovascular risk factors and/or events.

Over the past decade, multiple studies examined cardiac changes in CKD, especially using 5/6 Nx to induce CKD, however, the results are highly variable [11]. In fact, several studies reported that the mere induction of CKD induced the development of cardiac hypertrophy and even failure [14,28], while others observed more mild alterations to even no clear cardiac effects [29,30]. This may be related to the use of different mouse strains and methods of CKD induction, but also to differences in reported parameters. Clinically, uremic cardiomyopathy is characterized by myocardial changes as LV hypertrophy, fibrosis and cardiac dysfunction [3,31]. For example, LV hypertrophy, as occurring in 30% of CKD stage 2–4 patients and 70–80% of patients with end-stage kidney disease (CKD stage 5D), is mainly driven by increased cardiac pre- and/or afterload as well as pathophysiological changes in intracellular mediators and plays a characteristic role in cardiac remodeling and dysfunction [3]. Furthermore, CKD is associated with systemically enhanced levels of oxidative stress and inflammation [31]. However, studies mostly do not report on all these parameters and mainly focus on selected pathophysiological processes. Also, our recent systematic review and meta-analysis revealed that different readouts of a pathophysiological process or cardiac function may be differentially affected within one study, so that lack of consistent parameter reporting complicates clear comparison of different studies and CKD models [11]. This is also the case for development of uremic cardiomyopathy in C57BL/6 mice [11], the mouse strain mostly used for genetic modifications and thus mechanistic studies. Our comparative study exactly aimed to compare cardiac function and morphology in different experimental CKD models and protocols in a more systematic approach, with a main focus on adenine-induced nephropathy.

First, our study reveals that the protocol of adenine-induced CKD needs to be adapted based on the mouse strain and diet used. Whereas supplementing a standard diet with 0.2% adenine could trigger initial kidney damage in C57BL/6J wild-type mice after two weeks, C57BL/6J *ApoE*$^{-/-}$ mice fed a high-fat diet supplemented with 0.2% adenine did not demonstrate signs of kidney dysfunction in this time frame. Instead, a 0.3% (10 days induction)/0.15% (maintenance) adenine concentration was required in *ApoE*$^{-/-}$ mice on high-fat diet to induce sufficient kidney damage (Model 5).

Secondly, excluding models with insufficient kidney damage (Model 4; C57BL/6J mice 6 weeks on 0.2%/0.05% adenine diet) or those that had be ended prematurely due to extensive body-weight loss (Model 6; C57BL/6 N mice 11 weeks on 0.3%/0.2% adenine diet), three models developed an at least moderate chronic kidney dysfunction with >1.5-fold rise in serum creatinine, >2.5-fold rise in serum urea and kidney fibrosis (Models 5, 7, 8; Fig. 1). Of note, CKD enhanced oxidative stress markers in the heart in each of these models, with increased cardiac levels of heme oxygenase-1 (HO-1) and/or 8-hydroxy-2′-

deoxyguanosine (8-OHdG) (Fig. 1B). Increased numbers of 8-OHdG$^+$ nuclei in the heart were previously also reported in a mouse model of transversal aortic constriction (TAC) [12] and diabetic cardiomyopathy [32]. HO-1, a cytoprotective enzyme that degrades pro-oxidant heme [33], is induced upon cellular oxidative stress and therefore frequently used as biomarker thereof. For example, increased HO-1 in heart tissue was observed in a mouse model of TAC [34] as well as in rats subjected to 5/6 Nx and hyperuricemia [35]. Among underlying mechanisms of increased oxidative stress responses in CKD, uremic toxin accumulation may promote inflammation or initiation of endothelial nitric oxide synthase uncoupling, and therefore superoxide production in animal models [36].

Our findings of increased oxidative stress responses are in line with and extend recent observations of increased signs of cardiac inflammation in adenine-fed mice (C57BL/6 [37]; 129/Sv [38]). However, we did not observe the clinical phenotype of uremic cardiomyopathy with a clearly reduced cardiac function and development of cardiac hypertrophy as displayed in patients with advanced CKD [3], neither did we detect clear cardiac interstitial fibrosis. Of note, all investigated models in this study displayed at most a moderate to moderate-severe CKD for a maximum of 16 weeks (not taking into account model 6 that had to be excluded from further analysis due to extensive body-weight loss). Since patients in advanced CKD stage are exposed to severe kidney dysfunction for long time periods, mouse models with prolonged severe CKD might still be able to drive cardiac remodeling. Furthermore, in the clinical context, additional cardiovascular risk factors might considerably add to the vulnerability of the heart in terms of cardiac fibrosis, hypertrophy and dysfunction. In the context of experimental models, the few previous studies examining cardiac effects of adenine-induced CKD did report on the development of hypertension [37,39], cardiac hypertrophy [40] and fibrosis [39] within 4–8 weeks upon CKD induction in C57BL/6 mice. Hypertension was also reported in 129/Sv mice upon 8 weeks of adenine-treatment [38]. Whether hypertension might have increased adenine-mediated effects on the heart in the previously reported studies remains to be further examined.

In contrast to adenine induced-CKD, 5/6 Nx has been more frequently applied to study CKD effects on the heart. 129/Sv mice revealed to be more prone to develop hypertension and cardiac hypertrophy upon 5/6 Nx compared to C57BL/6 [11] and developed cardiac fibrosis from 4 weeks after 5/6 Nx [11,38,41–44]. Cardiac fibrosis and hypertrophy were also detected 12 weeks after 5/6 Nx in 129/Sv but not in C57BL/6JRj in a direct strain comparison, and although in this study, both mouse strains displayed hypertension upon 5/6 Nx, the 129/Sv strain developed more severe kidney damage as well as albuminuria compared to C57BL/6JRj [45]. Combined, this suggests that the degree of kidney damage, and potentially hypertension, contribute to the higher susceptibility of the 129/Sv strain to CKD-induced cardiac effects. In line, in the C57BL/6 5/6 Nx models we studied, CKD only induced a moderate effect on heart function for the mouse model with prolonged mild CKD and a CKD-mediated blood pressure increase (Model 3), though without induction of cardiac hypertrophy or fibrosis. Others previously identified cardiac functional impairments before the onset of cardiac hypertrophy or fibrosis, which suggested cardiac hypertrophy to rather develop as a secondary, potentially initial compensatory effect in response to initial cardiac dysfunction, though with risk of developing in progressive cardiac damage and failure in later stages [44,46].

To provide further insights into CKD-induced cardiac changes on a molecular level, RNA-sequencing was performed on cardiac tissue of adenine-fed 129/Sv mice compared to sham animals (Model 8). This revealed molecular alterations in inflammatory and oxidative stress responses (with increases in *Depp1, Ddit4, Ager, Sphk1, Rgcc, Gpnmb, Cebpb, Acp5*) as well as processes related to extracellular matrix and fibrosis (with increased *Ager, Rgcc, Col8a2, Mmp12, Gpnmb*; decreased *Snca, Spon2, Apln, Smoc2, Mmp15*). Upregulated pathophysiological mediators included mediators of ROS, oxidative stress and/or inflammation (e.g. DEPP1 [15], DDIT4 [16], AGER [18], SPHK1 [19], RGCC [47]) as well as inducers of ECM production and organ fibrosis (e.g. AGER [23], RGCC [22], COL8A2 [24], MMP12 [25]). Increased GPNMB levels have previously also been observed in the stressed heart upon infarction [48], chronic β-adrenergic stimulation or pressure overload [49]. Also a downregulation of cardioprotective genes may contribute to a pathophysiological maladaptation of the heart in CKD, as e.g. for SNCA counteracting organ fibrosis [50], or for SPON2 and APLN being protective against AngII- and/or pressure overload-induced cardiac dysfunction and pathological remodeling [51,52]. On the other hand, molecular profiling also pointed to processes counteracting fibrosis (e.g. decreased SMOC) [27] and ROS/inflammation (e.g. increased ACP5 [20]; decreased hemoglobin alpha (HBA-A1, HBA-A2) and ALAS2 *(data not shown)* as rate-limiting enzyme in heme synthesis [53]).

All combined, 129/Sv mice on adenine-induced CKD revealed an increased cardiac oxidative stress response characterized by an increase in ROS-inducing mediators and a decrease in cardioprotective mediators, as well as an increased level of the oxidative stress markers HO-1 and 8-OHdG (Fig. 7). Since depending on its source, dose and duration, oxidative stress can induce either protective signaling events or detrimental effects with rather maladaptive consequences that can lead to cardiac dysfunction and failure [54], and since cardiac function was largely preserved in the investigated models, it is presently unclear whether the observed molecular responses in the heart predispose to the development of heart failure or rather offer protection. Furthermore, also protective anti-inflammatory feedback responses were detected. Similarly, both pro-as well as anti-fibrotic responses were observed on a molecular level, which could contribute to the observation that no general cardiac interstitial fibrosis developed in our CKD models.

We conclude that overall, it is challenging to develop a mouse model of CKD with a clearly dysfunctional cardiac phenotype. Since several weeks of at least moderate CKD do not necessarily induce cardiac dysfunction nor substantial structural remodeling, it needs to be critically questioned whether additional "hits" are required to induce uremic cardiomyopathy with cardiac dysfunction and remodeling. This is in line with our recent systematic review of CKD/CVD animal models, which concluded that genetic factors as well as additional cardiovascular risk factors, such as hypertension, can increase the susceptibility of the heart to CKD-induced damage [11]. Whether by the induction of oxidative stress and inflammation, the heart is predisposed (i.e., at risk) or rather preconditioned (i.e., protected) from maladaptive cardiac remodeling needs to be explored by future studies that add a second stressor to CKD, such as pressure overload, myocardial infarction or metabolic dysfunction (i.e., obesity and/or diabetes).

All experimental mouse models in this study were performed with male mice. It would be of great interest to perform further experiments including both male and female mice to evaluate potential sex-specific differences. Furthermore, CKD induction was performed in relatively young mice. Because of the relation between aging and both CKD and CVD, a potential impact of aging on the extent of kidney-heart crosstalk is possible. Additional experiments with aged mice would be a possibility, as well as a further prolongation of the adenine diet beyond the longest CKD duration in our study (being 16 weeks).

Of note, although our CKD models did not develop cardiac interstitial fibrosis, mice with prolonged moderate to severe kidney dysfunction developed myocardial calcified deposits surrounded by fibrotic tissue, as detected in 129/Sv after 13 weeks of adenine-feeding (Model 8) as well as in C57BL/6 N mice with severe kidney dysfunction induced by prolonged high adenine-diet (Model 6) (Fig. 1B). Myocardial calcifications, which are expected to contribute to cardiac dysfunction when excessive, have also been detected in patients with chronic kidney failure [55,56], in whom they might even be highly underdiagnosed since they could be detected in 59% of cardiac tissues of dialysis patients during autopsy [57]. However, the etiology and mechanisms of these calcifications remain currently unclear.

In summary, our comprehensive and comparative study of adenine-induced CKD mouse models reveals that the induction of several weeks of at least moderate CKD does not necessarily induce cardiomyopathy. This casts doubts upon a simple mono-causal concept of uremic cardiomyopathy and suggests that additional "hits" are required to induce clear cardiac dysfunction and remodeling in CKD. Overall, CKD altered oxidative stress responses in the heart and enhanced cardiac oxidative stress markers, in a diverse spectrum of mouse models. Whether this provides a certain degree of cardioprotection or in fact increases the risk of enhanced cardiovascular damage upon additional cardiovascular risk factors and/or events, will be addressed in future studies.

## Declaration of competing interest

CM received honoraria for consulting and/or speeches from AstraZeneca, Bayer, Berlin Chemie, Boehringer Ingelheim, Novo Nordisk, Novartis, Pfizer, Servier. The other authors report that no conflict of interest exists.

## Data availability

Data will be made available on request.

## Funding and Acknowledgements

This research was supported by the German Research Foundation (DFG SFB/TRR219 Project-ID 322900939). H.N. was furthermore supported by the Else Kröner-Fresenius-Stiftung (Project 2020_EKEA.60). H. N. and J.J. also received support of DFG SFB 1382 (project-ID 403224013) and from the European Union's Horizon 2020 research and innovation programme under the Marie Skłodowska-Curie grant agreement No 764474 (CaReSyAn). E.P.C.v.d.V. was supported by a grant from the Interdisciplinary Center for Clinical Research within the faculty of Medicine at the RWTH Aachen University, the DZHK (German Centre for Cardiovascular Research) and the BMBF (German Ministry of Education and Research), and NWO-ZonMw Veni (91619053). P.B. was also supported by the DFG (Project-ID 454024652, 432698239 and 445703531), the European Research Council (ERC; Consolidator Grant AIM.imaging.CKD, No 101001791) and the BMBF (STOP-FSGS-01GM1901A). C.M. was and is supported by DFG SFB 894 and Ma2528/7-1, the Corona Foundation and the Barth Syndrome Foundation. Transgenic mice (roGFP2-Orp1) were originally imported and kindly provided by Dr. Tobias Dick (German Cancer Research Center – DKFZ, Germany). Scanning of histological slides was performed by Dr. Anja Scheller (Department of Physiology, Saarland University, Germany). We thank Josefin Soppert for support with the animal experiment application and Ellen Becker, Julia Weber, Sandra Janku, Ivo Sluijsmans, Melanie Garbe, Stefanie Elbin, Yuan Kong and Roya Soltan for their technical support.

## Appendix A. Supplementary data

Supplementary data to this article can be found online at https://doi.org/10.1016/j.redox.2022.102459.

## References

[1] N.R. Hill, S.T. Fatoba, J.L. Oke, J.A. Hirst, C.A. O'Callaghan, D.S. Lasserson, F. D. Hobbs, Global prevalence of chronic kidney disease - a systematic review and meta-analysis, PLoS One 11 (2016), e0158765.

[2] G. Manjunath, H. Tighiouart, H. Ibrahim, B. MacLeod, D.N. Salem, J.L. Griffith, J. Coresh, A.S. Levey, M.J. Sarnak, Level of kidney function as a risk factor for atherosclerotic cardiovascular outcomes in the community, J. Am. Coll. Cardiol. 41 (2003) 47–55.

[3] J. Jankowski, J. Floege, D. Fliser, M. Böhm, N. Marx, Cardiovascular disease in chronic kidney disease: pathophysiological insights and therapeutic options, Circulation 143 (2021) 1157–1172.

[4] R.W. Major, M.R.I. Cheng, R.A. Grant, S. Shantikumar, G. Xu, I. Oozeerally, N. J. Brunskill, L.J. Gray, Cardiovascular disease risk factors in chronic kidney disease: a systematic review and meta-analysis, PLoS One 13 (2018), e0192895.

[5] A. Ortiz, A. Covic, D. Fliser, D. Fouque, D. Goldsmith, M. Kanbay, F. Mallamaci, Z. A. Massy, P. Rossignol, R. Vanholder, A. Wiecek, C. Zoccali, G.M. London, Epidemiology, contributors to, and clinical trials of mortality risk in chronic kidney failure, Lancet (London, England) 383 (2014) 1831–1843.

[6] H. Noels, M. Lehrke, R. Vanholder, J. Jankowski, Lipoproteins and fatty acids in chronic kidney disease: molecular and metabolic alterations, Nat. Rev. Nephrol. 17 (2021) 528–542.

[7] M. Tonelli, P. Muntner, A. Lloyd, B.J. Manns, S. Klarenbach, N. Pannu, M.T. James, B.R. Hemmelgarn, Risk of coronary events in people with chronic kidney disease compared with those with diabetes: a population-level cohort study, Lancet (London, England) 380 (2012) 807–814.

[8] H. Noels, P. Boor, C. Goettsch, M. Hohl, W. Jahnen-Dechent, V. Jankowski, I. Kindermann, R. Kramann, M. Lehrke, D. Linz, C. Maack, B. Niemeyer, L.P. Roma, K. Schuett, T. Speer, S. Wagenpfeil, C. Werner, S. Zewinger, M. Böhm, N. Marx, J. Floege, D. Fliser, J. Jankowski, The new SFB/TRR219 research Centre, Eur. Heart J. 39 (2018) 975–977.

[9] T. Jia, H. Olauson, K. Lindberg, R. Amin, K. Edvardsson, B. Lindholm, G. Andersson, A. Wernerson, Y. Sabbagh, S. Schiavi, T.E. Larsson, A novel model of adenine-induced tubulointerstitial nephropathy in mice, BMC Nephrol. 14 (2013) 116.

[10] B.M. Klinkhammer, S. Djudjaj, U. Kunter, R. Palsson, V.O. Edvardsson, T. Wiech, M. Thorsteinsdottir, S. Hardarson, O. Foresto-Neto, S.R. Mulay, M.J. Moeller, W. Jahnen-Dechent, J. Floege, H.J. Anders, P. Boor, Cellular and molecular mechanisms of kidney injury in 2,8-dihydroxyadenine nephropathy, J. Am. Soc. Nephrol. : JASN (J. Am. Soc. Nephrol.) 31 (2020) 799–816.

[11] J. Soppert, J. Frisch, J. Wirth, C. Hemmers, P. Boor, R. Kramann, S. Vondenhoff, J. Moellmann, M. Lehrke, M. Hohl, E.P.C. van der Vorst, C. Werner, T. Speer, C. Maack, N. Marx, J. Jankowski, L.P. Roma, H. Noels, A systematic review and meta-analysis of murine models of uremic cardiomyopathy, Kidney Int. 101 (2) (2022) 256–273.

[12] A.G. Nickel, A. von Hardenberg, M. Hohl, J.R. Löffler, M. Kohlhaas, J. Becker, J. C. Reil, A. Kazakov, J. Bonnekoh, M. Stadelmaier, S.L. Puhl, M. Wagner, I. Bogeski, S. Cortassa, R. Kappl, B. Pasieka, M. Lafontaine, C.R. Lancaster, T.S. Blacker, A. R. Hall, M.R. Duchen, L. Kästner, P. Lipp, T. Zeller, C. Müller, A. Knopp, U. Laufs, M. Böhm, M. Hoth, C. Maack, Reversal of mitochondrial transhydrogenase causes oxidative stress in heart failure, Cell Metabol. 22 (2015) 472–484.

[13] J. Soppert, M. Lehrke, N. Marx, J. Jankowski, H. Noels, Lipoproteins and lipids in cardiovascular disease: from mechanistic insights to therapeutic targeting, Adv. Drug Deliv. Rev. 159 (2020) 4–33.

[14] J.E. Kieswich, J. Chen, S. Alliouachene, P.W. Caton, K. McCafferty, C. Thiemermann, M.M. Yaqoob, A novel model of reno-cardiac syndrome in the C57BL/6 mouse strain, BMC Nephrol. 19 (2018) 346.

[15] S. Salcher, M. Hermann, U. Kiechl-Kohlendorfer, M.J. Ausserlechner, P. Obexer, C10ORF10/DEPP-mediated ROS accumulation is a critical modulator of FOXO3-induced autophagy, Mol. Cancer 16 (2017) 95.

[16] S. Qiao, M. Dennis, X. Song, D.D. Vadysirisack, D. Salunke, Z. Nash, Z. Yang, M. Liesa, J. Yoshioka, S. Matsuzawa, O.S. Shirihai, R.T. Lee, J.C. Reed, L.W. Ellisen, A REDD1/TXNIP pro-oxidant complex regulates ATG4B activity to control stress-induced autophagy and sustain exercise capacity, Nat. Commun. 6 (2015) 7014.

[17] M.T. Coughlan, D.R. Thorburn, S.A. Penfold, A. Laskowski, B.E. Harcourt, K. C. Sourris, A.L. Tan, K. Fukami, V. Thallas-Bonke, P.P. Nawroth, M. Brownlee, A. Bierhaus, M.E. Cooper, J.M. Forbes, RAGE-induced cytosolic ROS promote mitochondrial superoxide generation in diabetes, J. Am. Soc. Nephrol. : JASN (J. Am. Soc. Nephrol.) 20 (2009) 742–752.

[18] G. Daffu, C.H. del Pozo, K.M. O'Shea, R. Ananthakrishnan, R. Ramasamy, A. M. Schmidt, Radical roles for RAGE in the pathogenesis of oxidative stress in cardiovascular diseases and beyond, Int. J. Mol. Sci. 14 (2013) 19891–19910.

[19] N. Takuwa, S. Ohkura, S. Takashima, K. Ohtani, Y. Okamoto, T. Tanaka, K. Hirano, S. Usui, F. Wang, W. Du, K. Yoshioka, Y. Banno, M. Sasaki, I. Ichi, M. Okamura, N. Sugimoto, K. Mizugishi, Y. Nakanuma, I. Ishii, M. Takamura, S. Kaneko, S. Kojo, K. Satouchi, K. Mitumori, J. Chun, Y. Takuwa, S1P3-mediated cardiac fibrosis in sphingosine kinase 1 transgenic mice involves reactive oxygen species, Cardiovasc. Res. 85 (2010) 484–493.

[20] A.J. Bune, A.R. Hayman, M.J. Evans, T.M. Cox, Mice lacking tartrate-resistant acid phosphatase (Acp 5) have disordered macrophage inflammatory responses and reduced clearance of the pathogen, Staphylococcus aureus, Immunology 102 (2001) 103–113.

[21] A.J. Mouton, O.J. Rivera Gonzalez, A.R. Kaminski, E.T. Moore, M.L. Lindsey, Matrix metalloproteinase-12 as an endogenous resolution promoting factor following myocardial infarction, Pharmacol. Res. 137 (2018) 252–258.

[22] W.Y. Huang, Z.G. Li, H. Rus, X. Wang, P.A. Jose, S.Y. Chen, RGC-32 mediates transforming growth factor-beta-induced epithelial-mesenchymal transition in human renal proximal tubular cells, J. Biol. Chem. 284 (2009) 9426–9432.

[23] J. Zhao, R. Randive, J.A. Stewart, Molecular mechanisms of AGE/RAGE-mediated fibrosis in the diabetic heart, World J. Diabetes 5 (2014) 860–867.

[24] B. Skrbic, K.V. Engebretsen, M.E. Strand, I.G. Lunde, K.M. Herum, H.S. Marstein, I. Sjaastad, P.K. Lunde, C.R. Carlson, G. Christensen, J.L. Bjørnstad, T. Tønnessen, Lack of collagen VIII reduces fibrosis and promotes early mortality and cardiac dilatation in pressure overload in mice, Cardiovasc. Res. 106 (2015) 32–42.

[25] L. Stawski, P. Haines, A. Fine, L. Rudnicka, M. Trojanowska, MMP-12 deficiency attenuates angiotensin II-induced vascular injury, M2 macrophage accumulation, and skin and heart fibrosis, PLoS One 9 (2014), e109763.

[26] Y. Yuting, F. Lifeng, H. Qiwei, Secreted modular calcium-binding protein 2 promotes high fat diet (HFD)-induced hepatic steatosis through enhancing lipid deposition, fibrosis and inflammation via targeting TGF-β1, Biochem. Biophys. Res. Commun. 509 (2019) 48–55.
[27] C. Gerarduzzi, R.K. Kumar, P. Trivedi, A.K. Ajay, A. Iyer, S. Boswell, J. N. Hutchinson, S.S. Waikar, V.S. Vaidya, Silencing SMOC2 ameliorates kidney fibrosis by inhibiting fibroblast to myofibroblast transformation, JCI insight 2 (2017).
[28] C.Y. Lin, Y.J. Hsu, S.C. Hsu, Y. Chen, H.S. Lee, S.H. Lin, S.M. Huang, C.S. Tsai, C. C. Shih, CB1 cannabinoid receptor antagonist attenuates left ventricular hypertrophy and Akt-mediated cardiac fibrosis in experimental uremia, J. Mol. Cell. Cardiol. 85 (2015) 249–261.
[29] M.B. Thomsen, M.S. Nielsen, A. Aarup, L.S. Bisgaard, T.X. Pedersen, Uremia increases QRS duration after β-adrenergic stimulation in mice, Physiological reports 6 (2018), e13720.
[30] E.L. Clinkenbeard, M.L. Noonan, J.C. Thomas, P. Ni, J.M. Hum, M. Aref, E. A. Swallow, S.M. Moe, M.R. Allen, K.E. White, Increased FGF23 protects against detrimental cardio-renal consequences during elevated blood phosphate in CKD, JCI insight 4 (2019).
[31] N. Kaesler, A. Babler, J. Floege, R. Kramann, Cardiac remodeling in chronic kidney disease, Toxins 12 (2020).
[32] X. He, Q. Ma, Disruption of Nrf2 synergizes with high glucose to cause heightened myocardial oxidative stress and severe cardiomyopathy in diabetic mice, J. Diabetes Metabol. Suppl 7 (2012).
[33] N.G. Abraham, A. Kappas, Heme oxygenase and the cardiovascular-renal system, Free Radic. Biol. Med. 39 (2005) 1–25.
[34] C. Chen, R. Huo, Y. Tong, Y. Sheng, H.B. Liu, X. Gao, O. Nakajima, B.F. Yang, D. L. Dong, Systemic heme oxygenase-1 transgenic overexpression aggravates pressure overload-induced cardiac hypertrophy in mice, Cell. Physiol. Biochem. : international journal of experimental cellular physiology, biochemistry, and pharmacology 28 (2011) 25–32.
[35] H. Omizo, Y. Tamura, C. Morimoto, M. Ueno, Y. Hayama, E. Kuribayashi-Okuma, S. Uchida, S. Shibata, Cardio-renal protective effect of the xanthine oxidase inhibitor febuxostat in the 5/6 nephrectomy model with hyperuricemia, Sci. Rep. 10 (2020) 9326.
[36] K. Daenen, A. Andries, D. Mekahli, A. Van Schepdael, F. Jouret, B. Bammens, Oxidative stress in chronic kidney disease, Pediatr. Nephrol. 34 (2019) 975–991.
[37] A. Nemmar, S. Al-Salam, S. Beegam, N.E. Zaaba, J. Yasin, N. Hamadi, B.H. Ali, Cardiac inflammation, oxidative stress, Nrf2 expression, and coagulation events in mice with experimental chronic kidney disease, Oxid. Med. Cell. Longev. 2021 (2021), 8845607.
[38] F. Sakata, Y. Ito, M. Mizuno, A. Sawai, Y. Suzuki, T. Tomita, M. Tawada, A. Tanaka, A. Hirayama, A. Sagara, T. Wada, S. Maruyama, T. Soga, S. Matsuo, E. Imai, Y. Takei, Sodium chloride promotes tissue inflammation via osmotic stimuli in subtotal-nephrectomized mice, Lab. Invest. 97 (2017) 432–446.
[39] F. Nanto-Hara, Y. Kanemitsu, S. Fukuda, K. Kikuchi, K. Asaji, D. Saigusa, T. Iwasaki, H.J. Ho, E. Mishima, T. Suzuki, C. Suzuki, T. Tsukimi, T. Matsuhashi, Y. Oikawa, Y. Akiyama, S. Kure, Y. Owada, Y. Tomioka, T. Soga, S. Ito, T. Abe, The guanylate cyclase C agonist linaclotide ameliorates the gut-cardio-renal axis in an adenine-induced mouse model of chronic kidney disease, Nephrol. Dial. Transplant. : official publication of the European Dialysis and Transplant Association - European Renal Association 35 (2020) 250–264.
[40] Y. Huang, S. Wang, J. Zhou, Y. Liu, C. Du, K. Yang, X. Bi, M. Liu, W. Han, K. Wang, J. Xiong, S. Wang, Y. Wang, L. Nie, C. Liu, D. Zhang, J. Gu, C. Zeng, J. Zhao, IRF1-mediated downregulation of PGC1α contributes to cardiorenal syndrome type 4, Nat. Commun. 11 (2020) 4664.
[41] J. Elkareh, S.M. Periyasamy, A. Shidyak, S. Vetteth, J. Schroeder, V. Raju, I. M. Hariri, N. El-Okdi, S. Gupta, L. Fedorova, J. Liu, O.V. Fedorova, M.B. Kahaleh, Z.J. Xie, D. Malhotra, D.K. Watson, A.Y. Bagrov, J.I. Shapiro, Marinobufagenin induces increases in procollagen expression in a process involving protein kinase C and Fli-1: implications for uremic cardiomyopathy, Am. J. Physiol. Ren. Physiol. 296 (2009) F1219–F1226.
[42] A.M. Siedlecki, X.H. Jin, A.J. Muslin, Uremic cardiac hypertrophy is reversed by rapamycin but not by lowering of blood pressure, Kidney Int. 75 (2009) 800–808.
[43] J. Xie, J. Yoon, S.W. An, M. Kuro-o, C.L. Huang, Soluble klotho protects against uremic cardiomyopathy independently of fibroblast growth factor 23 and phosphate, J. Am. Soc. Nephrol. 26 (2015) 1150–1160.
[44] P.D. Winterberg, R. Jiang, J.T. Maxwell, B. Wang, M.B. Wagner, Myocardial dysfunction occurs prior to changes in ventricular geometry in mice with chronic kidney disease (CKD), Physiological reports 4 (2016).
[45] M. Hamzaoui, Z. Djerada, V. Brunel, P. Mulder, V. Richard, J. Bellien, D. Guerrot, 5/6 nephrectomy induces different renal, cardiac and vascular consequences in 129/Sv and C57BL/6JRj mice, Sci. Rep. 10 (2020) 1524.
[46] J. O'Sullivan, S.L. Finnie, O. Teenan, C. Cairns, A. Boyd, M.A. Bailey, A. Thomson, J. Hughes, C. Bénézech, B.R. Conway, L. Denby, Refining the mouse subtotal nephrectomy in male 129S2/SV mice for consistent modeling of progressive kidney disease with renal inflammation and cardiac dysfunction, Front. Physiol. 10 (2019) 1365.
[47] X.B. Cui, J.N. Luan, K. Dong, S. Chen, Y. Wang, W.T. Watford, S.Y. Chen, RGC-32 (response gene to complement 32) deficiency protects endothelial cells from inflammation and attenuates atherosclerosis, Arterioscler. Thromb. Vasc. Biol. 38 (2018) e36–e47.
[48] A. Järve, S. Mühlstedt, F. Qadri, B. Nickl, H. Schulz, N. Hübner, C. Özcelik, M. Bader, Adverse left ventricular remodeling by glycoprotein nonmetastatic melanoma protein B in myocardial infarction, Faseb. J. : official publication of the Federation of American Societies for Experimental Biology 31 (2017) 556–568.
[49] L.Y. Lin, S. Chun Chang, J. O'Hearn, S.T. Hui, M. Seldin, P. Gupta, G. Bondar, M. Deng, R. Jauhiainen, J. Kuusisto, M. Laakso, J.S. Sinsheimer, A. Deb, C. Rau, S. Ren, Y. Wang, A.J. Lusis, J.J. Wang, A. Huertas-Vazquez, Systems genetics approach to biomarker discovery: GPNMB and heart failure in mice and humans, G3 (Bethesda, Md) 8 (2018) 3499–3506.
[50] M. Bozic, M. Caus, R.R. Rodrigues-Diez, N. Pedraza, M. Ruiz-Ortega, E. Garí, P. Gallel, M.J. Panadés, A. Martinez, E. Fernández, J.M. Valdivielso, Protective role of renal proximal tubular alpha-synuclein in the pathogenesis of kidney fibrosis, Nat. Commun. 11 (2020) 1943.
[51] Z.Y. Bian, X. Wei, S. Deng, Q.Z. Tang, J. Feng, Y. Zhang, C. Liu, D.S. Jiang, L. Yan, L.F. Zhang, M. Chen, J. Fassett, Y. Chen, Y.W. He, Q. Yang, P.P. Liu, H. Li, Disruption of mindin exacerbates cardiac hypertrophy and fibrosis, J. Mol. Med. (Berl.) 90 (2012) 895–910.
[52] T. Sato, A. Kadowaki, T. Suzuki, H. Ito, H. Watanabe, Y. Imai, K. Kuba, Loss of apelin augments angiotensin II-induced cardiac dysfunction and pathological remodeling, Int. J. Mol. Sci. 20 (2019).
[53] A. Khechaduri, M. Bayeva, H.C. Chang, H. Ardehali, Heme levels are increased in human failing hearts, J. Am. Coll. Cardiol. 61 (2013) 1884–1893.
[54] D. Weissman, C. Maack, Redox signaling in heart failure and therapeutic implications, Free Radic. Biol. Med. 171 (2021) 345–364.
[55] J. Martín-Cuartero, D. Yagüe-Romeo, E. Abril-Avellanas, [Myocardial calcification in chronic renal failure], Rev. Esp. Cardiol. 60 (2007) 1092.
[56] A.E. Kempf, M.G. Momeni, F. Saremi, Myocardial calcinosis in chronic renal failure, J. Radiol. Case Rep. 3 (2009) 16–19.
[57] D.C. Kuzela, W.E. Huffer, J.D. Conger, S.D. Winter, W.S. Hammond, Soft tissue calcification in chronic dialysis patients, Am. J. Pathol. 86 (1977) 403–424.